

AC CALORIMETRY APPLIED TO POWDERED SAMPLES

Simulation and tests

M. Barrio, J. Font, J. Muntasell and J. Ll. Tamarit

DEPARTAMENT DE FÍSICA I ENGINYERIA NUCLEAR, UNIVERSITAT POLITÈCNICA DE CATALUNYA, DIAGONAL 647, 08028 BARCELONA, SPAIN

(Received March 29, 1990; in revised form April 5, 1990)

This paper reports a home-made AC calorimeter designed for C_p measurements on powdered samples. The results of tests with SiC and Al₂O₃ at constant temperature demonstrated that it is possible to measure C_p for powdered samples with the same accuracy as for substances usually analysed by AC calorimetry (liquids and single-crystals).

The results obtained with the AC method agreed with those determined with the inverse filtering technique. This indicates that this technique is also suitable for C_p measurements at constant temperature or with a very low scanning rate.

The experimental system was simulated by a localized-constant model (RC model). This model allows analysis of the range of frequency and scanning rate values appropriate for the measurements.

AC calorimetry has usually been applied for C_p measurements on liquids [1-3] and single-crystals [4-6]. This technique has been employed for substances with very different thermal conductivities (metals [7,8] and liquid-crystals [1, 9]) measurements being made at constant temperature [10] or at low scanning rates [9, 11]. In this paper we present an AC calorimetric system for C_p determinations on powdered samples, which allows measurements with temperature programming.

The experimental device was simulated by means of a localized-constant model (RC model). RC models with constant parameters have been widely used to analyse AC calorimetric systems [10-12]. In these models, one considers a heat capacity coupled to a thermostat whose temperature remains constant. This kind of simulation requires a much simpler mathematical analysis than that corresponding to the models based on the Fourier equation (one-dimensional heat flux models [13, 14] employed to study AC calorimetric systems).

John Wiley & Sons, Limited, Chichester
Akadémiai Kiadó, Budapest

In this work we also report the results of calibration tests with SiC and Al₂O₃, and compare them with those obtained by inverse filtering [15-17].

Simulation of the experimental system

In this work, we consider an RC model with a heat capacity $C(t)$ at temperature T , coupled to a thermostat whose temperature, T_b , increases linearly as a function of time. The scheme of the model is given in Fig. 1. P is the thermal conductance of the link to the thermostat and β is the scanning rate.

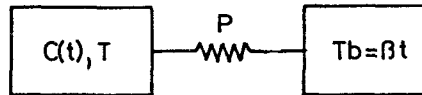


Fig. 1 Scheme of the RC mode of our simulation

This work is a continuation of a previous study [18] in which the heat capacity variation in calorimeters with temperature programming was analysed.

System response to AC power signal

The balance equation for an AC power signal, \dot{Q} , introduced to an element of heat capacity $C(t)$, is

$$\dot{Q} = \dot{Q}_{dc} + \dot{Q}_{ac} \sin(2\pi ft) = C(t) \frac{dT}{dt} + P(T - T_b) \quad (1)$$

\dot{Q}_{dc} being the continuous compound of the signal \dot{Q} , \dot{Q}_{ac} the amplitude of the alternating compound and f the frequency.

In order to analyse the system response, we considered a linear heat capacity variation:

$$C(t) = \dot{C}t + C_0 \quad (2)$$

Taking into account Eq. (2) and putting $T_b = \beta t$, Eq. (1) may be rewritten as:

$$\dot{Q} = \dot{Q}_{dc} + \dot{Q}_{ac} \sin(2\pi ft) = (\dot{C}t + C_0) \frac{dT}{dt} + P(T - \beta t) \quad (3)$$

In order to obtain the temperature T , we solved Eq. (3) numerically by the Runge-Kutta method. We used simulation parameters corresponding to those of our experimental system. Figure 2 shows the variations of T during 40 periods of the signal \dot{Q} , for the following values of these parameters:

$$\begin{aligned} C_0 &= 0.5 \text{ J/deg} & \dot{C} &= 8 \cdot 10^{-5} \text{ J/(deg}\cdot\text{s)} & P &= 2 \cdot 10^{-2} \text{ W/deg} \\ \beta &= 8 \cdot 10^{-5} \text{ deg/s} & \dot{Q}_{dc} = \dot{Q}_{ac} &= 4 \cdot 10^{-4} \text{ W} & f &= 16 \text{ mHz} \end{aligned} \quad (4)$$

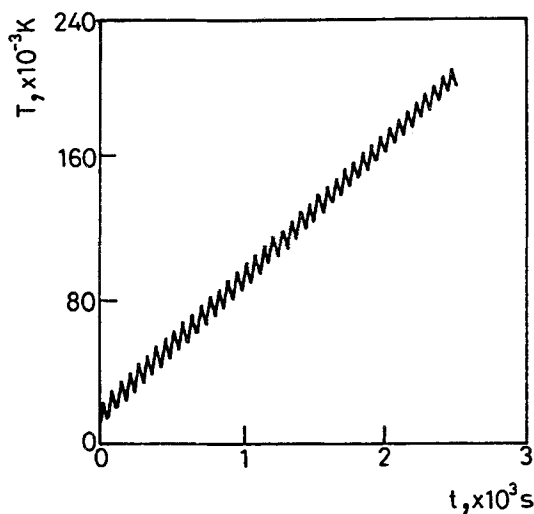


Fig. 2 Evolution of the temperature T as a function of time, obtained from the simulation done, using the parameters values given in (4)

This Figure shows that, out of the transient period, the temperature T oscillates, rising overall. The oscillation is due to the alternating compound of \dot{Q} , and the rise to the continuous compound of \dot{Q} and to the heating of the thermostat. In order to obtain the temperature term due to the alternating compound, we determined the minima and maxima of T by means of a programed algorithm. The adjustment of the average of the consecutive minima and maxima to a 3rd degree polynomial gives an equation corresponding to the temperature rise. From the difference between T and the equation

of the adjustment, we obtained the alternating compound, T_{ac} of T . Figure 3 presents T_{ac} as a function of t for the values of the simulation parameters indicated in (4).

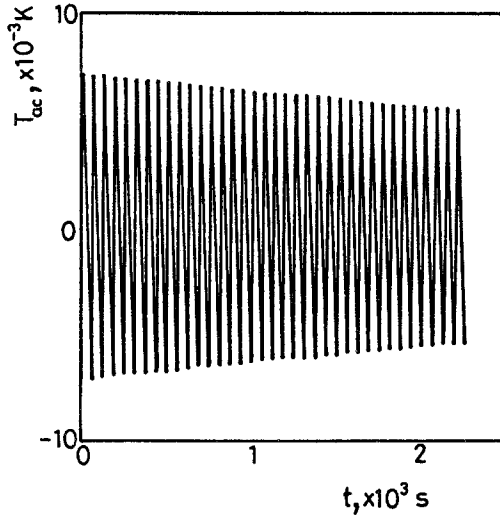


Fig. 3 Evolution of the altern compound of T as a function of time, determined from equations of the model, with the parameters values given in (4)

Figure 3 shows the decrease in the oscillation amplitude, ΔT_{ac} , due to the increase in the heat capacity with time.

We analysed the variation in T , given by the RC model, when the heat capacity $C(t)$ is constant ($C(t) = C$). Under these conditions, Eq. (3) has an analytical solution:

$$T = A \exp(-Pt/C) + \frac{\dot{Q}_{dc}}{P} + \beta(t - C/P) + \frac{\dot{Q}_{ac} \sin(\omega t - \Phi)}{(P^2 + \omega^2 C^2)^{1/2}} \quad (5)$$

ω being the angular frequency and Φ the angular phase difference between the alternating compounds of \dot{Q} and T , the expression of which is:

$$\Phi = \tan^{-1}(\omega C/P) \quad (6)$$

The integration constant A in Eq. (5) was determined by taking into account the fact that the temperatures of the element and the thermostat are

equal at $t = 0$ ($T(0) = T_b(0) = 0$). We obtained the following expression for A :

$$A = \frac{\beta C}{P} - \frac{\dot{Q}_{dc}}{P} + \frac{\dot{Q}_{ac} \sin \Phi}{(P^2 + w^2 C^2)^{1/2}} \quad (7)$$

The expression of the oscillation amplitude of T is

$$\Delta T_{ac} = \frac{\dot{Q}_{ac}}{(P^2 + w^2 C^2)^{1/2}} \quad (8)$$

For each frequency f , the thermal conductance P (determined in a previous calibration) and the AC power introduced to the sample, by using Eq. (8) we can obtain the value of the heat capacity C from ΔT_{ac} measurements. One must consider that C is the sum of the heat capacities of the sample, C_s , and the addenda, C_{add} , so the value of C_{add} must be determined in the calibration of the experimental system.

By using Eq. (8), we obtain Eq. (9), which shows the existence of a linear function between $(1/\Delta T_{ac})^2$ and C^2 :

$$\frac{1}{\Delta T_{ac}^2} = \frac{w^2}{\dot{Q}_{ac}^2} C^2 + \frac{P^2}{\dot{Q}_{ac}^2} \quad (9)$$

We checked if the same kind of function is also applicable in the simulation when the heat capacity changes in time. In Fig. 4, we represent $(1/\Delta T_{ac})^2$ as a function of $C(t)^2$ for the values of the simulation parameters indicated in (4).

The linear adjustment of the values presented in Fig. 4 gives the following results:

$$\frac{1}{\Delta T_{ac}^2} = 63219 C(t)^2 + 2455 \quad (10)$$

$r = 0.99995$, ΔT_{ac} being in K and $C(t)$ in J/deg.

If we compare Eq. (10) with Eq. (9), corresponding to the simulation at constant heat capacity, and using the values of w , \dot{Q}_{ac} and P indicated in (4), we can see differences smaller than 2% and 0.1% for the coefficients of linear and independent terms, respectively. The agreement between these

results justifies the utilization of Eq. (9) for systems with variable heat capacity, taking the ΔT_{ac} value corresponding to each value of C for the determination of this capacity. We have studied the limits in the values of the simulation parameters which allow application of the numerical method with good accuracy to obtain ΔT_{ac} values.

a) Influence of β

We have repeated this study for different values of β . We have verified that for the parameters values shown in (4), according to those of our experimental device, β cannot exceed $4 \cdot 10^{-4}$ deg/s. Over this limit, we cannot detect the oscillations of T because they are too small with respect to the dc rise temperature.

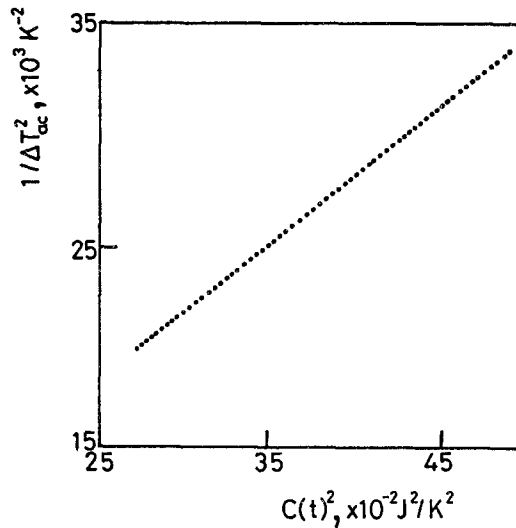


Fig. 4 Evolution of $(1/\Delta T_{ac})^2$ values vs. $C(t)^2$, obtained with the simulation parameters indicated in (4)

b) Influence of \dot{Q} and P

Tests with the model in which \dot{Q} and P are varied show that an increase of \dot{Q} or a decrease of P gives greater values of ΔT_{ac} . However, high values of \dot{Q} are not advisable because the continuous compound of T also increases.

When the thermal conductance P is small, the values of the oscillation amplitude are greater and, as proved by one-dimensional heat flux models [13, 14], the frequency range available for the measurements is wider.

c) Influence of f

Equation (9) shows that, for higher frequencies, the system is more sensitive to the changes in heat capacity. However, we must take into account the existence of an upper limit for f , fixed by the thickness and the thermal diffusivity of the sample [13, 14]. The RC model of our simulation cannot explain the loss of linearity of the representation of $(1/\Delta T_{ac})^2$ as a function of ω^2 , with values of f too high, because these experimental parameters (thickness and thermal diffusivity) are not considered in this kind of simulation.

System response to a constant power signal

In order to analyse whether the inverse filtering technique is suitable for C_p determinations, we have considered the above simulation with constant heat capacity when a constant power signal, \dot{Q}_o , is applied to the sample. The balance equation corresponding to this case is

$$\dot{Q}_o = C \frac{dT}{dt} + P (T - \beta t) \quad (11)$$

Its solution is

$$T = A \exp(-Pt/C) + \frac{\dot{Q}_o}{P} + \beta (t - C/P) \quad (12)$$

From the initial condition, $T(0) = T_b(0) = 0$, we obtain the expression of the integration constant A :

$$A = \frac{\beta C}{P} - \frac{\dot{Q}_o}{P} \quad (13)$$

Without power signal and out of the transient period corresponding to the start of heating of the system, the temperature T' of the capacity C varies according to the following equation:

$$T' = \beta t - \beta C/P \quad (14)$$

We define the system response ΔT as the difference between the temperature T and its value, T' , when no power is released. The expression for ΔT is

$$\Delta T = T - T' = T - \beta t + \beta C / P \quad (15)$$

By substitution of Eq. (12) into Eq. (15), when the steady state has been reached ($A \cdot \exp(-Pt/C) \rightarrow 0$), we obtain

$$\Delta T_{\max} = \dot{Q}_o / P = \dot{Q}_o \cdot S \quad (16)$$

where $S = 1/P$ is the sensitivity of the system [15]. Equation (11) may be rewritten as

$$\dot{Q}_o = P \left(T + \frac{C}{P} \frac{dT}{dt} - \beta t \right) \quad (17)$$

With the ΔT expression given in Eq. (15), Eq. (17) is reduced to

$$\dot{Q}_o = P \left(\Delta T + \frac{C}{P} \frac{d\Delta T}{dt} \right) \quad (18)$$

As we have pointed out in a previous paper [15], Eq. (18) verifies the correct utilization of the inverse filtering with a sensitivity $S = 1/P$ and a time constant $\tau = C/P$. Deconvolution of the ΔT signal by inverse filtering enables us to obtain the value of τ . In order to determine the heat capacity of the sample, as in AC calorimetry, a previous calibration, using known heat capacities, will be necessary to calculate the values of P and C_{add} .

The time constant τ is obtained by deconvolution of the relaxation signal of the system from the level $\Delta T_{\max} = \dot{Q}_o / P$. The assumption of a constant heat capacity is fully justified if we take into account that our experimental system has been designed to make measurements at very low scanning rates. Thus, the change in temperature during the relaxation interval of ΔT is small, and heat capacity variations due to this change are therefore negligible.

Experimental design

For C_p measurements, we used a copper calorimeter with a mass of 10 kg. The temperature of the calorimeter was controlled with a Peter Huber model Unistat (0.1 deg resolution) programmable thermostatic bath that regulates the temperature of the ambient surrounding the calorimeter.

The sample was placed in an aluminum crucible (0.2 mm thickness, 1.2 cm internal diameter) and covered with a disk of the same material. The mass of the crucible with disk was 128.0 mg.

The power signal was applied to the sample by means of a constantan wire resistance. This resistance was situated outside the crucible, in contact with its bottom. The signal was generated by a Hewlett-Packard 8116A function generator, the minimum frequency of which was 1 mHz with 0.01 mHz resolution.

The temperature variations in the sample were detected by a Siemens thermistor, with 1 mm^2 contact surface, placed above the aluminum disk. The calibration of the thermistor was performed with a calibrated Pt-100 Ω resistance, in the interval 298-303 K, with a scanning rate of $5 \cdot 10^{-3}$ deg/min and a sampling period of 30 s. An exponential function was adjusted to the values obtained in this calibration. The result of the adjustment was

$$R = 9.14246 \cdot 10^{10} \exp(-4.5010 \cdot 10^{-2} T) \quad (19)$$

where R and T are in Ω and K, respectively.

The thermistor signal was measured with a Solartron 7061 multimeter (0.1 Ω resolution). Numerical data acquisition was performed with an Olivetti-M24 personal computer with IEEE-488 bus.

The experimental system was calibrated at constant temperature (301.0 ± 0.1 K) with different masses of SiC (49.2, 96.8, 158.7 and 195.4 mg). The specific heat of SiC at this temperature is 0.693 ± 0.014 J/(g·deg) [19]. In order to check the calibration results, they were used to determine the specific heat of masses of 53.5, 91.6, 157.6 and 194.9 mg of Al_2O_3 (previously calcined at 1273 K). The grain size of both substances was less than 40 μm . Samples were compacted into the crucible until a maximum thickness of 2 mm was obtained.

Because of the very low thermal conductivity of our samples, power signals of small frequency, in the range 2-16 mHz, were used for AC calorimetry.

Results and discussion

In order to determine C_p values from the oscillation amplitudes via Eq. (9) by AC calorimetry, it is necessary to know the values of parameters \dot{Q}_{ac} and P . The purpose of the calibration with SiC was to obtain these.

First of all, we analysed the range of frequencies available for our measurements. We represented $(1/\Delta T_{ac})^2$ as a function of ω^2 for each mass of SiC and for different frequencies between 2 and 16 mHz. As an example, Fig. 5 shows the representation corresponding to a SiC mass of 195.4 mg.

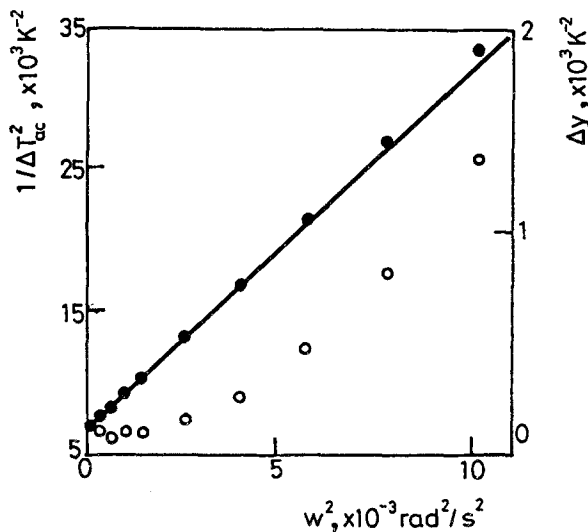


Fig. 5 Representation of $(1/\Delta T_{ac})^2$ experimental values (\bullet) vs. ω^2 , corresponding to a mass of SiC of 195.4 mg. Regression line and differences Δy (\circ) between $(1/\Delta T_{ac})^2$ experimental values and calculated from the adjustment are also included

The linear adjustments made for this function using the values corresponding to the frequencies up to 6 mHz gave values of the regression coefficient, r , varying between 0.99995 and 0.99999, the values of this coefficient being less than 0.99990 for frequencies in the range 8-16 mHz. Figure 5 also depicts the regression line obtained in the adjustment of the experimental values of $(1/\Delta T_{ac})^2$ corresponding to frequencies of 2, 3, 4, 5 and 6 mHz, and the differences between the experimental values of $(1/\Delta T_{ac})^2$ and those obtained from the adjustment, for all the frequencies used.

The loss of linearity as the frequency increases is more marked for large sample masses, because the influence of the thickness of the sample is higher under these conditions [13, 14]. Accordingly, we used frequencies of 2, 3, 4, 5 and 6 mHz for calibration.

Equation (9) leads to Eqs (20) and (21), which allow determination of \dot{Q}_{ac} and P :

$$\dot{Q}_{ac} = \frac{C}{a^{1/2}} = \frac{C_{add} + m_s c_s}{a^{1/2}} \quad (20)$$

$$P = C \frac{b^{1/2}}{a^{1/2}} = (C_{add} + m_s c_s) \frac{b^{1/2}}{a^{1/2}} \quad (21)$$

where c_s is the specific heat of the sample, m_s is its mass and a and b are the slope and the constant term, respectively, of the regression line corresponding to the adjustment of $(1/\Delta T_{ac})^2$ vs. w^2 .

Table 1 gives the values of $a^{1/2}$ obtained for each mass of SiC used.

Table 1 Values of $a^{1/2}$ for the different masses of SiC analysed

m_s , mg	$m_s c_s$, J/K	$a^{1/2}$, s/K
49.2	0.034	1446±15
96.8	0.067	1524±14
158.7	0.110	1617±15
195.4	0.135	1692±14

The value of $a^{1/2}$ corresponding to the measurement with the empty crucible is 1346 ± 6 s/deg. The average value of $b^{1/2}$ (independently of the sample mass, according to our model) for all the masses of SiC is 45.2 ± 0.5 deg⁻¹. Taking into account Eq. (20), we can calculate \dot{Q}_{ac} and C_{add} from the adjustment of $a^{1/2}$ vs. C_s . Figure 6 shows this adjustment.

By this method we obtained the values $\dot{Q}_{ac} = (40 \pm 1) \cdot 10^{-5}$ W and $C_{add} = 0.545 \pm 0.011$ J/deg. The regression coefficient of this adjustment is 0.999. This value may be considered acceptable since different masses of SiC were used for its determination and the effect of replacement of the sample and crucible into the calorimeter is included in this determination. Equation (21) gave a value of P of $(182 \pm 6) \cdot 10^{-4}$ W/deg.

In order to check the results of our calibration, we applied it to determine the specific heat of Al₂O₃, using the values of \dot{Q}_{ac} and C_{add} obtained with SiC. The results for Al₂O₃ are included in Table 2.

Table 2 Values of $a^{1/2}$ and heat capacity, C_s , obtained for Al₂O₃ from the calibration results

m_s , mg	$a^{1/2}$, s/K	C_s , J/K
53.5	1444±10	0.037±0.005
91.6	1504±19	0.061±0.009
157.6	1632± 9	0.112±0.005
194.9	1756± 4	0.162±0.004

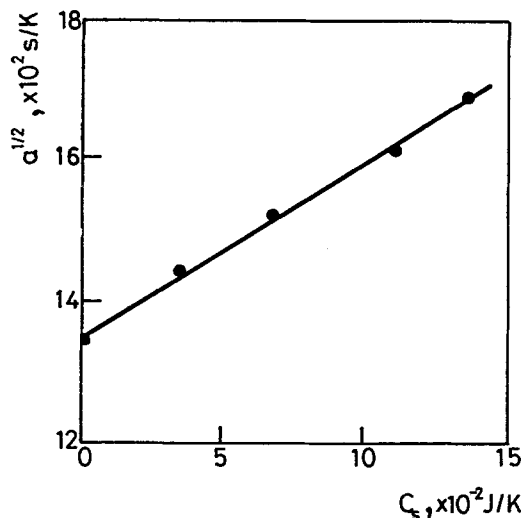


Fig. 6 Representation of $a^{1/2}$ as a function of the heat capacity, C_s , of the masses of SiC indicated in Table 1. Regression line of the adjustment is also included in this figure

These data gave $c_s = 0.73 \pm 0.07 \text{ J/(g} \cdot \text{deg)}$, in agreement with the value reported for Al_2O_3 at 301 K, $c_s = 0.779 \pm 0.023 \text{ J/(g} \cdot \text{deg)}$ [19].

We analysed the influence of the frequency on the sensitivity of our experimental system as the heat capacity changes. Table 3 gives the ΔT_{ac} values obtained for SiC with the lowest and highest frequencies used in our calibration. This Table also includes the oscillation amplitudes determined from the RC model with variable heat capacity and programming temperature.

Table 3 Experimental ($\Delta T_{ac} \text{ exp}$) and simulation ($\Delta T_{ac} \text{ mod}$) values of the oscillation amplitude obtained for SiC with the lowest and highest frequencies used

m_s	C_s	$f = 2 \text{ mHz}$		$f = 6 \text{ mHz}$	
		$\Delta T_{ac} \text{ exp.,}$ mK	$\Delta T_{ac} \text{ mod,}$ mK	$\Delta T_{ac} \text{ exp.,}$ mK	$\Delta T_{ac} \text{ mod,}$ mK
0	0.545	20.7±0.1	18.9	14.7±0.1	14.0
49.2	0.579	20.4±0.1	18.8	14.0±0.1	13.5
96.8	0.612	20.3±0.1	18.7	13.6±0.1	13.1
158.7	0.655	20.2±0.1	18.5	13.2±0.1	12.6
195.4	0.680	20.0±0.1	18.4	12.6±0.1	12.3

The differences between the experimental and simulation results are always smaller than 10 %. The agreement is better when the frequency is 6 mHz. We can also see in this Table that our experimental system is more sensitive to changes in heat capacity when higher frequencies are used. This fact was pointed out before from the simulation equation.

In order to analyse the applicability of the inverse filtering technique for C_p measurements, we applied a constant power signal to the sample, using the same masses of SiC. We determined the time constant $\tau = C/P$ by this technique. As an example, Fig. 7 shows the ΔT signal and the signal deconvoluted by inverse filtering with $\tau = 37.0$ s, for a sample mass of 195.4 mg.

The values of τ obtained for the different masses of SiC are included in Table 4. A sampling period of 0.5 s was used for numerical data acquisition.

Table 4 Time constants determined by inverse filtering, corresponding to the different masses of SiC analysed

m_s , mg	τ , s
49.2	32.0±0.5
96.8	33.5±0.5
158.7	35.5±0.5
195.4	37.0±0.5

The measurement with the empty crucible gave $\tau = 30.0 \pm 0.5$ s.

In order to calculate the heat capacity C_s of the sample from the inverse filtering results, it is necessary to determine previously the values of C_{add} and P for the experimental system. We can obtain these from the calibration, using the following equation:

$$\tau = (m_s C_s + C_{add})/P = (C_s + C_{add})/P \quad (22)$$

The linear adjustment of τ as a function of C_s enables us to determine C_{add} and P . In Fig. 8, τ is plotted vs. C_s for the values given in Table 4. This Figure also shows the regression line of this adjustment.

The regression coefficient of the adjustment is 0.999, which is equal to the value corresponding to the calibration by AC calorimetry. From the slope and the constant term of the regression line, we obtained $C_{add} = 0.597 \pm 0.030$ J/deg and $P = (20.0 \pm 1.1) \cdot 10^{-3}$ W/deg. The differences between these values and those determined with the AC method are about 10 %. Thus since margins of error of 10% are typical in C_p measurements by

AC calorimetry [2, 11], we can say that the results obtained by this technique and by inverse filtering are in agreement.

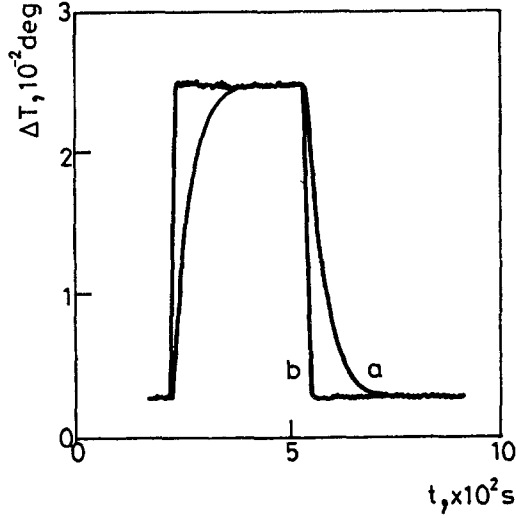


Fig. 7 Representation of the ΔT signal (a) and of the deconvoluted signal (b), with $\tau = 37.0$ s, corresponding to a mass of SiC of 195.4 mg

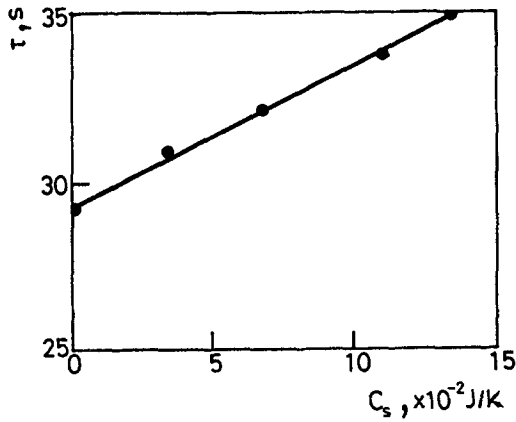


Fig. 8 Evolution of the time constant as a function of the heat capacity of SiC samples. Regression line of the adjustment is shown in this figure

Conclusions

The first results of the measurements made with our AC calorimeter, at constant temperature, show that it is possible to determine heat capacities of powdered samples with the same accuracy as in measurements with liquids or single-crystals. The characteristics of the calibration substances (size grain, thermal conductivity, compactness) must be as similar as possible to those of the samples whose specific heats are to be determined.

The studied RC model shows that measurements can be made by AC calorimetry with temperature programming, using very low scanning rates. Under these conditions, the time employed to analyse heat capacity variation with temperature is lower. Moreover, the control of the temperature in scanning mode is more accurate than in the steady state.

The simulation allows us to find a more adequate range of values of the experimental parameters for the measurements. Thus, for example, the simulation equations indicate that high frequencies are convenient, because the experimental system is then more sensitive to the changes in heat capacity. The calibration measurements demonstrate this fact. We must take into account the existence of an upper limit for the frequency values fixed by the characteristics of the samples (thickness and thermal conductivity). Moreover, a frequency increase causes a lowering of the oscillation amplitude. This fact also imposes an upper limit to the frequency range of the measurements.

Finally, we have verified that the inverse filtering is a technique that is readily applicable in measurements at constant temperature, and is also suitable for heat capacity determinations.

References

- 1 R. J. Birgeneau, C. W. Garland, G. B. Kasting and B. M. Ocko, *Phys. Rev. A* 24 (1981) 2624.
- 2 G. Sanchez, M. Meichle and C. W. Garland, *Phys. Rev., A* 28 (1983) 1647.
- 3 C. C. Huang and J. M. Viner, *Phys. Rev., A* 25 (1982) 3385.
- 4 J. D. Baloga and C. W. Garland, *Rev. Sci. Instrum.*, 48 (1977) 105.
- 5 C. W. Garland and J. D. Baloga, *Phys. Rev.*, B16 (1977) 331.
- 6 P. Schwartz, *Phys. Rev.*, B 4 (1971) 920.
- 7 P. Sullivan and G. Seidel, *Phys. Lett.*, 25A (1967) 229.
- 8 P. Handler, D. E. Mapother and M. Rayl, *Phys. Rev. Lett.*, 19 (1967) 356.
- 9 M. Meichle and C. W. Garland, *Phys. Rev.*, A27 (1983) 2624.
- 10 C. A. Schantz and D. L. Johnson, *Phys. Rev.*, A 17 (1978) 1504.
- 11 C. W. Garland, *Thermochim. Acta*, 88 (1985) 127.
- 12 G. B. Kasting, K. J. Lushington and C. B. Garland, *Phys. Rev.*, B 22 (1980) 321.
- 13 I. Hatta and A. J. Ikushima, *J. Appl. Phys. Jpn.*, 20 (1981) 1995.

- 14 S. Imaizumi, K. Suzuki and I. Hatta, *Rev. Sci. Instrum.*, 54 (1983) 1180.
- 15 E. Cesari, J. Font and J. Muntasell, *Thermochim. Acta*, 94 (1985) 387.
- 16 J. Sestak, *Thermophysical Properties of Solids. Their Measurements and Theoretical Thermal Analysis*, Academia Prague, 1984, p. 303.
- 17 J. Font, J. Muntasell, J. Navarro and E. Cesari, *Thermochim. Acta*, 88 (1985) 425.
- 18 J. Font, J. Muntasell, J. Navarro, J. Ll. Tamarit and E. Cesari, *Thermochim. Acta*, 118 (1987) 183.
- 19 J. H. Perry, *Chemical Engineers' Handbook* edited by McGraw-Hill Book Company, New York, 1974.

Zusammenfassung — Diese Arbeit beschreibt ein eigengefertigtes AC-Kalorimeter zur Messung von C_p an pulverisierten Proben. Die Ergebnisse der bei konstanten Temperaturen durchgeführten Tests mit SiC und Al₂O₃ zeigten, daß es möglich ist, C_p von pulverisierten Proben mit der AC-Kalorimetrie üblicherweise verwendeten Substanzen (Flüssigkeiten, Einkristalle)

Die mit der AC-Kalorimetrie erhaltenen Ergebnisse stimmten mit denen der inversen Filtrieretechnik überein. Dies zeigt, daß sich das Verfahren auch für C_p -Messungen bei konstanten Temperaturen oder bei sehr geringen Scanning-Geschwindigkeiten eignet.

Der Versuchsaufbau wurde durch ein Modell mit lokalisierten Konstanten (RC-Modell) simuliert. Dieses Modell ermöglicht eine Analyse des Frequenzbereiches und der für die Messungen günstigen Scanning-Geschwindigkeitswerte.